

# Adsorption of DNA on biomimetic apatites: Toward the understanding of the role of bone and tooth mineral on the preservation of ancient DNA



A. Grunenwald<sup>a,b</sup>, C. Keyser<sup>b</sup>, A.M. Sautereau<sup>a</sup>, E. Crubézy<sup>c</sup>, B. Ludes<sup>b</sup>, C. Drouet<sup>a,\*</sup>

<sup>a</sup> CIRIMAT Carnot Institute – Phosphates, Pharmacotechnics, Biomaterials, University of Toulouse, CNRS/INPT/UPS, ENSIACET, 4 allée Emile Monso, 31030 Toulouse Cedex 4, France

<sup>b</sup> Institute of Legal Medicine, AMIS Laboratory, CNRS UMR 5288, University of Strasbourg, 11 rue Humann, 67085 Strasbourg Cedex, France

<sup>c</sup> Molecular Anthropology and Image Synthesis Laboratory (AMIS), CNRS UMR 5288, University of Toulouse, 37 allée Jules Guesde, 31000 Toulouse, France

## ARTICLE INFO

### Article history:

Received 11 October 2013

Received in revised form

10 December 2013

Accepted 11 December 2013

Available online 19 December 2013

### Keywords:

Nanocrystalline apatite

Hydroxyapatite

Ancient DNA

Polyelectrolyte adsorption

Temkin isotherm

Elovich

## ABSTRACT

In order to shed some light on DNA preservation over time in skeletal remains from a physicochemical viewpoint, adsorption and desorption of DNA on a well characterized synthetic apatite mimicking bone and dentin biominerals were studied. Batch adsorption experiments have been carried out to determine the effect of contact time (kinetics), DNA concentration (isotherms) and environmentally relevant factors such as temperature, ionic strength and pH on the adsorption behavior. The analogy of the nanocrystalline carbonated apatite used in this work with biological apatite was first demonstrated by XRD, FTIR, and chemical analyses. Then, DNA adsorption kinetics was fitted with the pseudo-first order, pseudo-second order, Elovich, Ritchie and double exponential models. The best results were achieved with the Elovich kinetic model. The adsorption isotherms of partially sheared calf thymus DNA conformed satisfactorily to Temkin's equation which is often used to describe heterogeneous adsorption behavior involving polyelectrolytes. For the first time, the irreversibility of DNA adsorption toward dilution and significant phosphate-promoted DNA desorption were evidenced, suggesting that a concomitant ion exchange process between phosphate anionic groups of DNA backbone and labile non-apatitic hydrogenphosphate ions potentially released from the hydrated layer of apatite crystals. This work should prove helpful for a better understanding of diagenetic processes related to DNA preservation in calcified tissues.

© 2013 Elsevier B.V. All rights reserved.

## 1. Introduction

Bone and tooth remains often represent the only – but also the best – biological materials available for deoxyribonucleic acids (DNA) typing in anthropology and may additionally be exploited in forensic sciences [1,2]. In ancient samples, DNA arising from degraded cells is generally strongly fragmented, with a mean size around 200 base pairs, and its amplification may be limited by the presence of substances persisting after purification, and inhibiting PCR [3]. Although hard tissue samples are commonly used as a source of ancient DNA sequences, the processes of ancient DNA preservation in these mineralized tissues have received little systematic attention, both regarding qualitative and quantitative aspects.

Calcium phosphate apatites are the main components of human bone and teeth. The physico-chemical features of enamel highly resemble those of stoichiometric hydroxyapatite  $\text{Ca}_{10}(\text{PO}_4)_6(\text{OH})_2$ , both in terms of crystallographic structure and composition. In contrast, bone and dentin minerals are composed of non-stoichiometric apatite nanocrystals. Several studies have shown the possibility to prepare, under close-to-physiological conditions (temperature, pH), synthetic analogs to biological apatites that mimic their physico-chemical characteristics [4–6]. For both biological specimens and biomimetic analogs, the surface of the nanocrystals was found to exhibit a structured but metastable non-apatitic hydrated layer [7–9], containing labile ions (e.g.  $\text{Ca}^{2+}$ ,  $\text{HPO}_4^{2-}$ ,  $\text{CO}_3^{2-}$ ...) leading to an exceptional surface reactivity, either in terms of ionic exchanges or of molecular adsorption [10–13]. Furthermore, the possibility to control, for synthetic biomimetic apatites, the maturation state of the nanocrystals was evidenced by modifying experimental conditions such as temperature, pH or maturation time in solution [7,14,15]. These findings then enable the preparation of samples mimicking either newly formed or mature bone mineral.

\* Corresponding author at: CIRIMAT Carnot Institute, ENSIACET, 4 allée Emile Monso, 31432 Toulouse Cedex 4, France. Tel.: +33 034 32 34 11; fax: +33 034 32 34 99.

E-mail address: [christophe.drouet@ensiacet.fr](mailto:christophe.drouet@ensiacet.fr) (C. Drouet).

The role of the mineral apatitic matrix, potentially acting as a physical and a chemical barrier against DNA deterioration (through microbiological activity and environmental factors) has been widely mentioned in the literature to explain the exceptional preservation of DNA in hard tissues [16–18]. In fact, even in the absence of bacterial attack, the decay of free DNA molecules in aqueous solutions is completely achieved over few thousand years, based on spontaneous hydrolysis [17]. The presence of ancient DNA in samples aged over 600 000 years appears then consistent with the hypothesis of an adsorption of DNA fragments on bone and tooth apatitic matrix, thus limiting the possibility of chemical degradation and the accessibility of bacteria and their enzymes [19].

In another context, the ability of hydroxyapatite to adsorb DNA has been shown since 1957 for chromatographic purposes, using phosphate solutions with a concentration gradient as mobile phase [20–22]. More recently, apatites and other calcium phosphates nanoparticles have been investigated as drug carriers to deliver genetic materials to eukaryotic cells [23,24]. Okasaki et al. [25] have also examined the crystal growth of hydroxyapatite in the presence of DNA and suggested an affinity binding phenomenon based upon electrostatic interaction between negatively charged phosphate groups of the backbone of DNA and calcium ions from the apatite surface.

However, in spite of these various applications, the chemical interaction between apatites and DNA is generally assumed *a priori*, without an in-depth understanding of the nature of the binding mechanism involved; moreover very few quantitative data were reported to-date on apatite/DNA interactions.

The adsorption of several biological (macro)molecules other than nucleic acids (e.g. bovine serum albumin and other proteins, antibiotics, amino acids...) on synthetic biomimetic apatites has on the contrary already been the object of various works [11,12,26–28]. Interestingly, adsorption processes on biomimetic apatites was found to involve in some cases more complex mechanisms than solely based on the deposition of the molecule on the surface of the solid phase: in some instances indeed, the release of surface ions was found to occur simultaneously to the adsorption process [11,29,30]. Moreover, considerable variations of adsorption parameters are bound to be observed depending on the physico-chemical characteristics of the apatite crystals.

Based on these considerations, we report in this contribution a first physico-chemical insight on the interaction between DNA and a biomimetic apatite mimicking bone and dentin biominerals, with the goal to explain the diagenetic persistence of DNA extracted from skeletal remains. This experimental model was aimed at determining adsorption and desorption features (using calf thymus DNA as model DNA), and at comparing the obtained data with reports dealing with other biological molecules.

## 2. Materials and methods

### 2.1. Synthesis of apatite analogous to dentin and bone mineral

A biomimetic carbonated apatite sample, referred to as hac-1w, was synthesized by double decomposition according to the procedure described by Rey et al. [8]. Briefly, a calcium nitrate  $\text{Ca}(\text{NO}_3)_2 \cdot 4\text{H}_2\text{O}$  solution (52.2 g in 750 ml of deionized water) was poured at room temperature ( $20^\circ\text{C}$ ) into a solution of ammonium hydrogenophosphate  $(\text{NH}_4)_2\text{HPO}_4$  and sodium bicarbonate  $\text{NaHCO}_3$  (90 g of each in 1500 ml of deionized water). The excess of phosphate in the second solution was used to buffer the pH of the solution at a close-to-physiological value, namely 7.2. Maturation in solution has then been carried out for 7 days (1 week). The pH of the medium was found to remain constant during the whole

maturation process. The suspension was then filtered on a Büchner funnel, thoroughly washed with deionized water, freeze-dried and stored in a freezer ( $-18^\circ\text{C}$ ) so as to avoid any alteration of the apatite nanocrystals.

The apatite powder was then sieved, and the size fraction in the range of 100–200  $\mu\text{m}$  was used for all further experiments (adsorption/desorption).

### 2.2. DNA

Adsorption and desorption experiments were performed with DNA solutions prepared from sheared calf thymus DNA solutions (Trevigen). According to the manufacturer, the concentration of the mother calf thymus DNA solution is provided at 10 mg/ml in TE buffer (10 mM Tris, 1 mM EDTA, pH 8) with a fragment size range of 500–1000 bp.

### 2.3. Physico-chemical characterization

The chemical composition of the apatite compound synthesized was determined from titrations carried out by complexometry for the determination of the calcium content, by spectrophotometry for the total phosphate content (determination of the sum of  $\text{PO}_4^{3-}$  and  $\text{HPO}_4^{2-}$  ions, using the phospho-vanado-molybdenic method [31]) and by coulometric method (UIC, Inc. CM 5014 coulometer with CM 5130 acidification unit) for the carbonate content.

The crystal structure of the samples was checked by powder X-ray diffraction using an Inel diffractometer CPS 120 and the monochromatic Co K $\alpha$  radiation ( $\lambda_{\text{Co}} = 1.78892 \text{ \AA}$ ).

The specific surface area,  $S_w$ , was determined using a five points BET method (nitrogen adsorption) on a Tristar II Micromeritics apparatus.

Fourier transform infrared (FTIR) analyses were performed on a Perkin Elmer 1700 spectrometer with a resolution of  $4 \text{ cm}^{-1}$ , using the KBr pellet method.

The amount of adsorbed DNA, at equilibrium, after adsorption experiments was drawn by comparison of the concentrations in DNA before and after adsorption, using the UV absorption of the band at ca. 260 nm followed by spectrophotometry (Thermo Scientific NanoDrop 2000c spectrophotometer).

The amounts of calcium and (inorganic) phosphate ions present in the supernatants after adsorption or desorption were titrated respectively by atomic absorption (ContrAA 300, Analytik Jena) and by spectrophotometry using the phospho-vanado-molybdenic method as mentioned above. Prior to these analyses, the residual DNA molecules present in the supernatants were removed by pretreatment in acidic medium and centrifugation.

### 2.4. Adsorption and desorption experiments

For all experiments, the amount of apatite powder and volume of DNA solution (in glass flasks) were kept constant at respectively 10 mg and 7.5 ml. DNA solutions were prepared at increasing concentrations ranging from 0 to 500  $\mu\text{g}$  DNA/ml, in deionized water. This concentration range has been chosen to remain in the linear zone of Beer Lambert Law and avoid high solution viscosity, which could interfere with adsorption processes.

Adsorption kinetics was followed, at room temperature and pH 7, over a period of 4 weeks with a DNA solution of intermediate concentration (160–195  $\mu\text{g}/\text{ml}$ ).

For the establishment of adsorption isotherms, experiments were carried out with various pH values (by adding either HCl 0.1 M or NaOH 0.1 M), ionic strengths (by adding KCl) and temperatures, under constant mild stirring. Then the mixture was centrifuged (20 min at 1850 g and the supernatant was retrieved by filtration with Acrodisc® syringe filters with nylon membrane

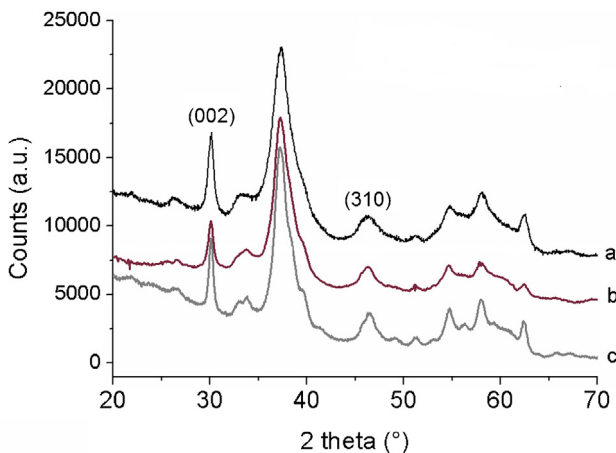


**Fig. 1.** XRD patterns ( $2\theta$  between  $20^\circ$  and  $70^\circ$ ) of (a) biomimetic carbonated apatite sample, hac-1w (maturation of 1 week), as compared to bone specimens: (b) rat (12 months), (c) human (man 57 y.o.).

( $0.45 \mu\text{m}$ , 25 mm). Each point was done in triplicate to check the reproducibility of our experimental model.

When mentioned in the text, the eventual desorption of pre-adsorbed DNA molecules was examined – in the same conditions of temperature and contact time as for the adsorption experiments – by investigating the effect of dilution by a factor 5, where 80 vol.% of the supernatant were replaced by deionized water, with or without addition of  $\text{KH}_2\text{PO}_4$  at a final concentration of 18 mM.

### 3. Results and discussion

#### 3.1. Physico-chemical characterization of apatite sample

The apatite sample hac-1w synthesized in this work was characterized by way of X-ray diffraction (XRD) analysis and Fourier-transform infrared (FTIR) spectroscopy.

The XRD pattern obtained (Fig. 1) was found to be characteristic of single-phased apatite, as no secondary crystallized phase was detected. A comparison with the patterns obtained on bone specimens, namely human femur (man, 57 y.o.) and rat bone (12 months old), as illustrated in Fig. 1, confirmed the biomimetic character of the hac-1w sample. As can be noted in all cases, the patterns exhibit the features of apatite with a rather low crystallinity state characteristic of biological apatites (except for tooth enamel). The application of Scherrer's formula to diffraction lines (002) and (310), leading respectively to an estimate of the mean length and width of the apatite crystals, gave mean crystallite dimensions of 15.7 nm length and 4.9 nm width. These values are clearly in the nanometer scale thus conferring an additional element in favor of the bone- or dentin-like character of this apatite compound.

The apatite nature of the sample was also confirmed by FTIR analysis (Fig. 2). Several differences could however, as expected, be evidenced by comparison to stoichiometric hydroxyapatite (HA). In particular, the presence of carbonate absorption bands was pointed out in the case of the sample hac-1w in the ranges  $1350$ – $1550 \text{ cm}^{-1}$  (assignable to the  $\nu_3(\text{CO}_3)$  vibration mode) and  $840$ – $910 \text{ cm}^{-1}$  (attributable to  $\nu_2(\text{CO}_3)$ ). In contrast, absorption bands at  $3572$  and  $632 \text{ cm}^{-1}$  typical of apatitic  $\text{OH}^-$  ions are not clearly detectable on the spectrum of hac-1w (see for example inset of Fig. 2). This observation indicates that this apatite sample is largely depleted in  $\text{OH}^-$  ions. This type of nonstoichiometry is common for biological apatites (e.g. [32]), and is typically accompanied by cationic vacancies (lack of calcium ions) and the substitution of  $\text{PO}_4^{3-}$  ions by divalent  $\text{HPO}_4^{2-}$  or  $\text{CO}_3^{2-}$ . Beside the already assessed presence of carbonate species in the apatite lattice, the existence of

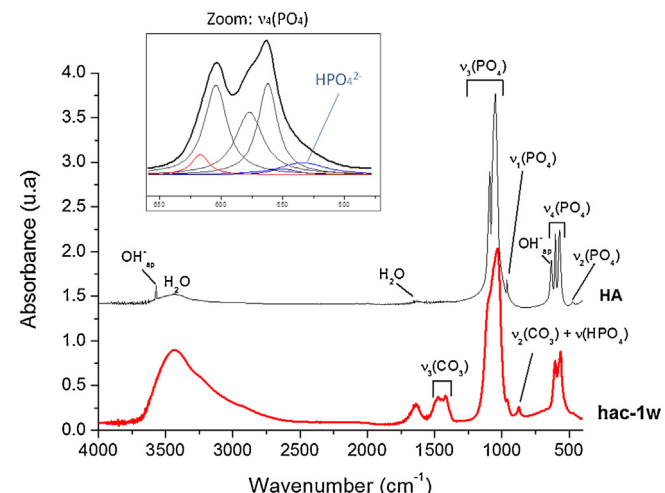


**Fig. 2.** FTIR spectra for biomimetic apatite (hac-1w) and for reference stoichiometric hydroxyapatite (HA) showing localization of apatitic hydroxyl ions, phosphates ions ( $\nu_1$ – $\nu_3$ ) and carbonates ions ( $\nu_2$ ,  $\nu_3$ , hac-1w only). Inset: spectral decomposition of the  $\nu_4(\text{PO}_4)$  vibration domain for hac-1w in the range  $400$ – $800 \text{ cm}^{-1}$ , revealing in particular the vibration of non-apatitic hydrogenphosphate labile ions.

$\text{HPO}_4^{2-}$  ions can indeed be established here on the basis of IR absorption appearing as a shoulder to the  $\nu_4(\text{PO}_4)$  bands, around  $535$ – $550 \text{ cm}^{-1}$  (see inset, Fig. 2).

The chemical composition of this apatite sample was then investigated. In particular, the  $\text{Ca}/(\text{P}+\text{C})$  molar ratio of the solid was determined from the chemical titration of calcium, carbonate and orthophosphate ions, leading to the value 1.36. This  $\text{Ca}/(\text{P}+\text{C})$  ratio is noticeably lower than 1.67, which is characteristic of stoichiometric HA, and this finding confirms the nonstoichiometry of this compound already suggested by FTIR analyses.

All the results reported above therefore assess the biomimetic character of the apatite sample hac-1w, with bone- or dentin-like characteristics, thus making of it an adequate substrate for DNA adsorption analyses in our context.

Taking into account the importance of the surface of apatite exposed to the DNA solution in adsorption experiments, the sample was sieved (between  $100$  and  $200 \mu\text{m}$ ) and the specific surface area of the resulting powder fraction was found to be of  $S_W = 180 \text{ m}^2/\text{g}$  as determined by nitrogen adsorption (BET measurement).

#### 3.2. Adsorption kinetics

The kinetics of adsorption of calf thymus DNA on the hac-1w biomimetic apatite sample prepared above was first followed, with the objective to determine experimental conditions allowing us to reach the thermodynamic equilibrium. To this aim, adsorption experiments were carried out (at room temperature and pH 7–7.5) starting from DNA solutions with a concentration in the range  $160$ – $195 \mu\text{g}/\text{ml}$ .

Fig. 3a reports the experimental data points by plotting the amount of DNA adsorbed, denoted  $N_{\text{ads}}$  (given in mg DNA/g of apatite), as a function of contact time and over a period of 4 weeks. This kinetic curve shows a steep increase of  $N_{\text{ads}}$  during the first day of contact between DNA molecules and the apatite substrate, followed by a progressive stabilization (up to about  $110$ – $120 \text{ mg DNA/g apatite}$  for this DNA concentration range). The analysis of the first derivative (see inset on Fig. 3a) allows one to examine in more details the variation of  $N_{\text{ads}}$  during the first 24 h of apatite/DNA contact. As can be seen, the vast majority of DNA molecules appear to be adsorbed within the first 2–3 h of contact – reaching coverage of the order of 70–80% (relatively to the maximum equilibrated adsorbed amount). These findings suggest that the adsorption process is not

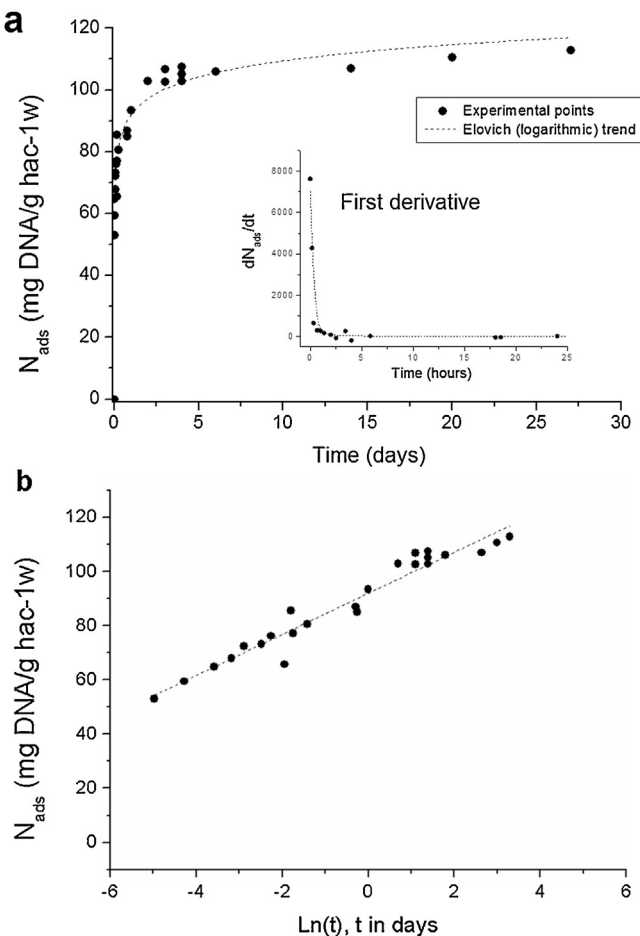


**Fig. 3.** Kinetics of DNA adsorption followed over 3 weeks at room temperature, neutral pH, on biomimetic apatite hac-1w. Adsorption is complete within 3 days, with a trend following Elovich's equation (dotted line): (a)  $N_{\text{ads}} = f(t)$ , inset: first derivative of first day data points showing that the adsorption process is almost complete within 3 h, (b) linear regression using Elovich's equation,  $N_{\text{ads}} = f(\ln(t))$ .

particularly hindered, during this first stage of adsorption, by steric hindrance of the DNA macromolecules at the surface of apatite nanocrystals. However, beyond this stage, such phenomena can probably contribute to the modification of slope observed (up to reaching thermodynamic equilibrium) and the rather slow evolution before final stabilization.

The shape of the adsorption kinetic curve  $N_{\text{ads}} = f(t)$  appears roughly with a logarithmic shape, and this type of variation was indeed confirmed by the rather good linearity ( $R^2 = 0.9463$ ) of the  $N_{\text{ads}} = f(\ln(t))$  plot as shown in Fig. 3b. Such a behavior is in particular representative of kinetic processes following Elovich's mathematical model [33]:

$$N_{\text{ads}} = \frac{1}{b} \ln(t + t_0) + \frac{1}{b} \ln(ab) \quad (1)$$

where " $t_0$ " (pre-Elovich period) is often found to be close to zero (which may reasonably be considered here taking into account the linearity found in Fig. 3b). This equation derives in fact from the description of the adsorption rate  $r_a = dN_{\text{ads}}/dt$ :

$$r_a = \frac{dN_{\text{ads}}}{dt} = a \cdot \exp(-b \cdot N_{\text{ads}}(t)) \quad (2)$$

Interestingly, the Elovich model was frequently considered to describe the kinetics of adsorption of (bio)molecules on heterogeneous surfaces [34,35], especially when the final stabilization is rather slow to occur (such as for example the case of the adsorption of hydrogen on mixed oxides [36]). Based on our findings, this

model thus appears to simulate rather well the adsorption of DNA on biomimetic apatite. A rather slow stabilization is indeed likely to happen here taking into account the length of the macromolecules of DNA and potential modifications of conformation upon adsorption.

Other kinetic models have however also been tested in this work in view of evaluating their potential pertinence. The general model proposed by Ritchie [37,38] was in particular tested, being based on an equation of the type:

$$\frac{d\theta}{dt} = k_n(1 - \theta)^n \quad (3)$$

where " $\theta$ " represents the coverage of the surface at time " $t$ ", and " $n$ " is the order of the reaction. Out of this general equation, two models are indeed often encountered in literature studies related to kinetics of adsorption, namely the pseudo-first order and pseudo-second order kinetic models:

$$N_{\text{ads}} = N_e \cdot [1 - \exp(-k_1 \cdot t)] \quad (\text{pseudo-first order}) \quad (4)$$

$$N_{\text{ads}} = N_e \cdot \left[ 1 - \left( \frac{1}{1 + k_2 \cdot t} \right) \right] \quad (\text{pseudo-second order}) \quad (5)$$

The application of these two types of equation to our experimental data however did not allow us to reach a satisfactory fit over the whole time range. In all cases, the fits obtained predicted a stabilization at significantly shorter contact times as compared to the experimental data. The use of a double-exponential model (DEM):

$$N_{\text{ads}} = N_e - a_1 \cdot \exp(-k_1 \cdot t) - a_2 \cdot \exp(-k_2 \cdot t) \quad (6)$$

proposed in the literature [39] for describing the rate of adsorption of two variants of nucleotides on montmorillonite also failed to simultaneously describe adequately the different stages of the kinetic adsorption curve observed in the present case (both for short and longer contact times).

The above findings thus suggest that the Elovich model remains the best model tested here, for describing satisfactorily the kinetics of adsorption of DNA macromolecules on biomimetic apatite.

### 3.3. Adsorption isotherm and desorption study

Taking into account the preceding kinetic data, the following sub-sections will aim at establishing DNA adsorption isotherms. On the basis of the above kinetics study, an apatite/DNA contact time of 3 days has been selected for all experiments. In a first stage, the isotherm relative to so-called "reference" conditions – namely room temperature, neutral pH and deionized water medium – was determined. In subsequent steps, the potential effects of pH, ionic strength and temperature were examined for deriving general tendencies on the adsorption process.

#### 3.3.1. Reference adsorption isotherm (room temperature, neutral pH, deionized water medium)

A reference adsorption isotherm was built by measuring the amount  $N_{\text{ads}}$  of DNA adsorbed (either given in  $\mu\text{g}/\text{mg}$  or in  $\mu\text{g}/\text{m}^2$ ) on the hac-1w carbonated nanocrystalline apatite sample (Fig. 4) as a function of the equilibrium concentration of DNA in the supernatant  $C_{\text{eq}}$  ( $\mu\text{g}/\text{ml}$ ). These experiments were carried out at room temperature ( $\sim 22^\circ\text{C}$ ), neutral pH (initial value close to 7.4) and in deionized water.

The profile of this  $N_{\text{ads}} = f(C_{\text{eq}})$  curve is typical of an adsorption isotherm plot tending toward a monolayer-like coverage, with a steep increase of the adsorbed amount over a narrow range in  $C_{\text{eq}}$  followed by the obtainment of a plateau (around  $N_m \approx 160 \text{ mg/g}$ ). It may be noted however that experimental datapoints show a

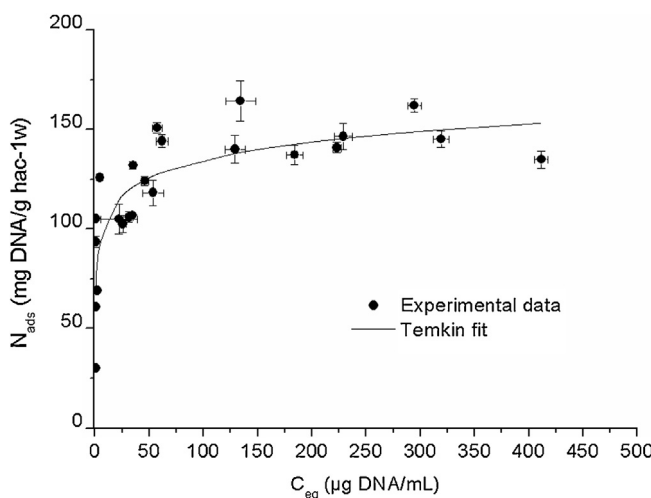


**Fig. 4.** The reference adsorption isotherm of calf thymus DNA (0.75–4.5 mg, initial concentration range 40–600 μg/ml) on biomimetic carbonated apatite hac-1w (10 mg) in standard conditions (room temperature, 3 days of incubation, neutral pH) fits with Temkin logarithmic curve (straight line)

rather high dispersion, which can be related to relative heterogeneity in DNA fragment lengths and apatite particle size (despite preliminary sieving). A dispersion of physico-chemical characteristics among biological apatites is however also naturally observed *in vivo* due to varying status in mineral remodeling/aging states. In addition, some variability in DNA fragment length also presumably occurs in *post mortem* events. Therefore, such experimental adsorption isotherms are expected to approximate reasonably well the variability of actual diagenetic phenomena.

In order to shed some more light on the type of adsorption behavior observed here between DNA molecules and biomimetic apatite crystals, several adsorption models were tested on the basis of mathematical linearization of the data. The Langmuir model as well as two derivatives, namely Freundlich and Temkin, were successively tested by plotting  $1/N_{\text{ads}} = f(1/C_{\text{eq}})$  for Langmuir (Eq. (7)),  $\ln(N_{\text{ads}}) = f(\ln(C_{\text{eq}}))$  for Freundlich (Eq. (8)) and  $N_{\text{ads}} = f(\ln(C_{\text{eq}}))$  for Temkin (Eq. (9)), referring to the isotherm equations:

$$N_{\text{ads}} = N_m \left( \frac{K_L \cdot C_{\text{eq}}}{1 + K_L \cdot C_{\text{eq}}} \right) \quad (7)$$

$$N_{\text{ads}} = K_F \cdot C_{\text{eq}}^{1/n} \quad (8)$$

$$N_{\text{ads}} = B \cdot \ln(A) + B \cdot \ln(C_{\text{eq}}) \quad (9)$$

where  $K_L$ ,  $N_m$ ,  $K_F$ ,  $n$ ,  $A$  and  $B$  are the corresponding constants (at fixed temperature).

After fitting our data to each of these three equations (see Table 1), only a poor fit was found with the Langmuir equation (correlation  $R^2$  coefficient ~0.20), thus strongly suggesting that the associated hypotheses of this model (unique heat of adsorption for all adsorption sites, no interaction between adsorbate molecules) do not strictly apply here. In contrast, a significantly better fit ( $R^2 > 0.5$ ) was found for the other two models, i.e. Freundlich and

Temkin, which take into account heterogeneous heats of adsorption (the latter being related to the local affinity of surface sites for specific molecular functional group). In particular, the best agreement was found with the Temkin model ( $R^2$  coefficient close to 0.67), which theoretically supposes a proportional variation of adsorption enthalpies as a function of the coverage. These results can be paralleled to literature results dealing with the adsorption of ionic adsorbents on heterogeneous surfaces [40–43], where Temkin isotherm was also often linked to an Elovich-type kinetic model.

Fig. 4 points out a situation where the maximal DNA coverage reached on our apatitic substrate hac-1w is close to 160 mg/g. Although it appears appealing to compare this adsorption parameter with reported values measured on apatites for other molecules, it should be reminded here that care should be taken for such comparisons since such substrates probably do not exhibit the same surface features, due to different synthesis histories. Indeed, it was previously suggested that the apatite maturation stage (leading to modified surface and bulk characteristics [15]) may have a direct significant influence on adsorption processes [11,12,26,29]. Also, when DNA macromolecules are involved, it appears difficult to express the adsorbed amounts in terms of moles (rather than grams) due to the polydispersity of the molecular weight of DNA fragments (typically in the range 10–1000 bp in our case). In the hypothesis of a sample made of an average of 500 bp, an approximated value for DNA molecular weight would be 330 kDa; therefore the measured  $N_m$  value of 160 mg/g would be equivalent to about 0.49 μmol/g. For information only, the maximum adsorbed amount of another macromolecule – bovine serum albumin – on a nanocrystalline apatite substrate (non-carbonated but with a rather similar maturation state) reached 11.4 μmol/g (764 mg/g) [12].

Based on a Temkin-like behavior, the logarithmic fit of experimental datapoints was added in Fig. 4. Although care should be taken at this stage for drawing conclusive statements on the distribution of surface sites for DNA adsorption, these findings suggest an evolution of the anchoring behavior of DNA macromolecules along the adsorption process (i.e. upon coverage increase), which may in turn be related to their 3D conformation(s).

### 3.3.2. Desorption study

In order to shed some more light on the adsorption mechanism for such DNA/apatite systems, the potential displacement of DNA macromolecules out of the apatitic surface (desorption) was investigated by following the effect of dilution on the residual adsorbed amount.

A first set of experiments was carried out by performing a dilution by a factor 5 in deionized water, and the results are reported on Fig. 5a. Interestingly, as is shown in this figure, the data essentially indicate the absence of desorption in such conditions. These findings may probably be paralleled with previous works on the adsorption of bisphosphonate on apatites [11,29] where the absence of desorption upon dilution was also evidenced (pointing out a non-reversible adsorption process associated to a genuine “anchoring” of the molecules on the surface of the substrate). In the case of bisphosphonates, this non-reversibility was related by the authors to the release of phosphate ions from the solid surface simultaneously to the molecular grafting process via a phosphate end-group.

In the present case, the lack of significant desorption upon dilution could possibly be related to a rather similar scenario, where anionic phosphate groups from the DNA backbone may interact with phosphate ions from the surface of the nanocrystals. Calcium and phosphate ions were titrated from adsorption supernatants (retrieved after adsorption experiments for various increasing values of  $C_{\text{eq}}$ ) as well as in a “blank” experiment carried out in similar conditions but in the absence of DNA. In all

**Table 1**

Adsorption parameters and correlation coefficients calculated according to the theoretical models tested in this work.

Adsorption model	Fitted adsorption parameters	Correlation coeff.
Langmuir	$N_m = 114.9 \text{ mg/g}$	$K_L = 3.0 \text{ ml}/\mu\text{g}$
Freundlich	$K_F = 74.66 \text{ mg/g} (\text{ml}/\mu\text{g})^n$	$n = 7.17$
Temkin	$A = 450.078 \text{ ml}/\mu\text{g}$	$B = 13.416$
		$R^2 = 0.201$
		$R^2 = 0.561$
		$R^2 = 0.671$

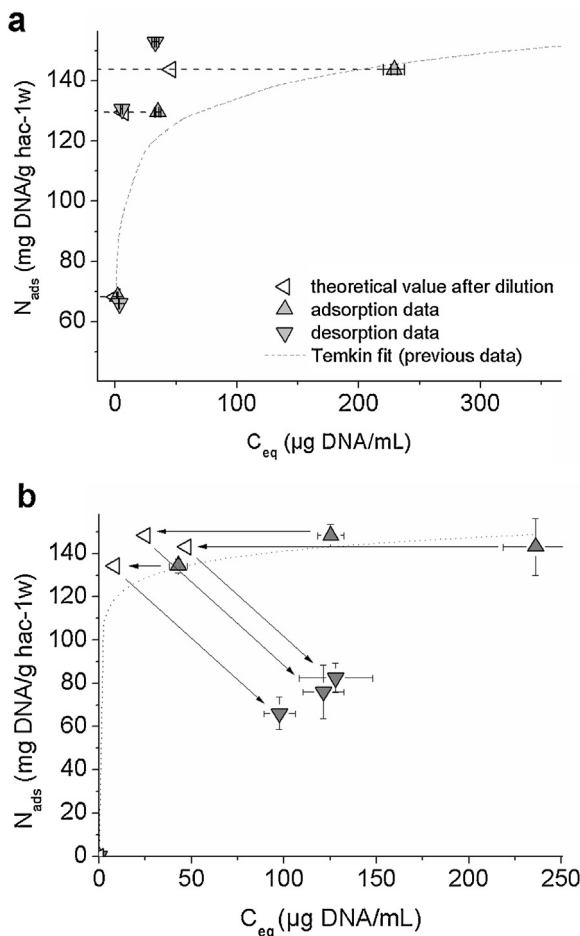


**Fig. 5.** Effect of dilution in (a) deionized water or (b) in the presence of phosphate ions ( $[P] = 18 \text{ mM}$ , pH 7, on the adsorption of DNA on biomimetic apatite. (a) After 3 d of adsorption, 80% of the solution was replaced with deionized water (dilution step) for 3 more days: the “desorption” data points do not follow the isotherm despite the dilution of the medium,  $N_{ads}$  remaining essentially unchanged for each point, indicating the quasi-absence of DNA desorption. (b) Same experiment with dilution by neutral phosphate solution. Partial desorption of ca. 30–50% of DNA is observed after 3 days.

cases, our results indicated the presence of both types of ions in solution, and in increasing amounts as a function of the adsorbed amount, with a concentration range of phosphorus and calcium in the supernatants, respectively between ca. 0.3–0.8 mmol/l and 0.4–1.3 mmol/l (data not shown). These findings could hypothetically be attributed to the (partial) dissolution of the apatitic substrate and/or to the release of ions from the surface due to the adsorption process itself. The concomitant presence of both calcium cations and phosphate anions, however, strongly supports at least some extent of apatite dissolution. At this point, it is difficult to differentiate between the two types of contributions (dissolution-related or adsorption-related); especially taking into account the non-congruence of dissolution processes for nonstoichiometric apatites [29,30].

Additional “desorption” tests were nonetheless run in the presence of phosphate ions in the medium (by addition of  $\text{KH}_2\text{PO}_4$ , see Section 2), while keeping the pH value neutral. Remarkably, in this case, the residual adsorbed amounts were systematically found to sharply decrease (Fig. 5b). This type of behavior was previously observed for example for bisphosphonates [44] where the adsorption process was accompanied by a release of phosphate ions. Taking all these statements in consideration, and although additional investigation dedicated to these aspects (e.g. to the

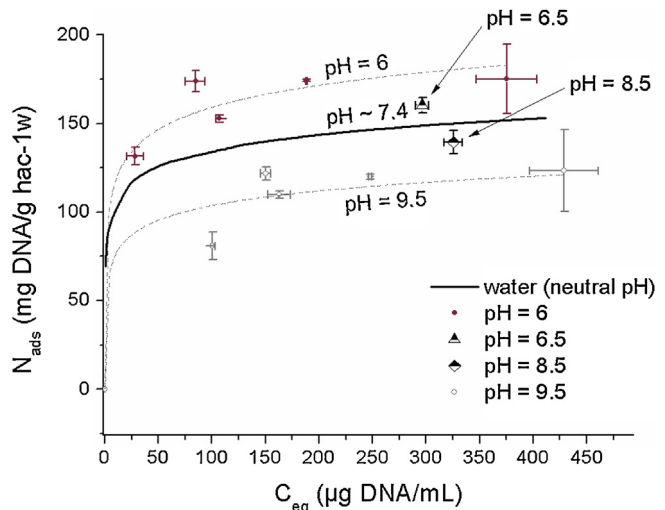


**Fig. 6.** Effect of pH on the adsorption process in standard conditions of DNA onto biomimetic nanocrystalline carbonated apatite ( $6 < \text{pH} < 9.5$ ).

incongruence of apatite dissolution) will be needed, our data suggest in the present case that phosphate ions compete with DNA molecules for surface sites of apatite crystals.

### 3.3.3. Effect of pH on DNA adsorption

The maximum adsorption amount  $N_m$  of DNA onto the poorly crystalline biomimetic apatite sample hac-1w was then followed (still at 22 °C) as a function of the initial pH of the medium (in the range 6–9.5). Indeed, pH may presumably play a non-negligible role in adsorption processes involving ionic crystals such as apatites. Also, pH may also vary upon *post mortem* conditions.

As shown in Fig. 6, the value of  $N_m$  was found to increase upon acidification (ca. +13% at pH 6) of the medium, and conversely to decrease upon alkalization (ca. -23% at pH 9.5). Several factors may potentially come into play for explaining this behavior. In particular, partial apatite (surface) dissolution is expected to increase upon acidification [45], thus modifying exposed surface characteristics. To a lesser extent, acidification could be seen as a means to facilitate the release of  $\text{HPO}_4^{2-}$  ions from the surface of apatite nanocrystals, as these ions are known to be the predominant form of phosphate ions on such surfaces [46,47]. In turn, such an increased mobility of  $\text{HPO}_4^{2-}$  ions could then facilitate the anchoring of DNA phosphate groups onto the surface of the crystals (see discussion in Section 3.3.2). Another potential explanation for this pH effect on  $N_m$  could be related to a change in DNA conformation upon acidification/alkalinization, thus modifying the profile of the grafted molecules. In contrast it appears that these pH effects may not be related to the speciation of the phosphate groups (main ionization site of double-stranded DNA) from the DNA backbone. Indeed, their  $pK_a$  value of ca. 1.5 [48] points to a situation where these phosphate groups are ionized for any  $\text{pH} > 1.5$ .

It is interesting to remark however that the experimental pH values of the media after adsorption (data not shown) showed the general tendency to evolve toward neutrality, independently of the initial pH value (whether acidic or alkaline). This effect may be both due (1) to a surface equilibration phenomenon of the apatite crystal surface and (2) to the adsorption process itself leading to phosphate ion release, as indicated in the previous sub-section. Indeed, the release of phosphate ions (which are mostly protonated on the surface of biomimetic apatites, namely either  $\text{HPO}_4^{2-}$  or  $\text{H}_2\text{PO}_4^-$ ) in a medium exhibiting a pH value between ca. 5 and 10 is expected to evolve toward neutralization due to the buffering effect of the  $\text{H}_2\text{PO}_4^-/\text{HPO}_4^{2-}$  acid-base couple ( $pK_a = 7.2$ ) [49].

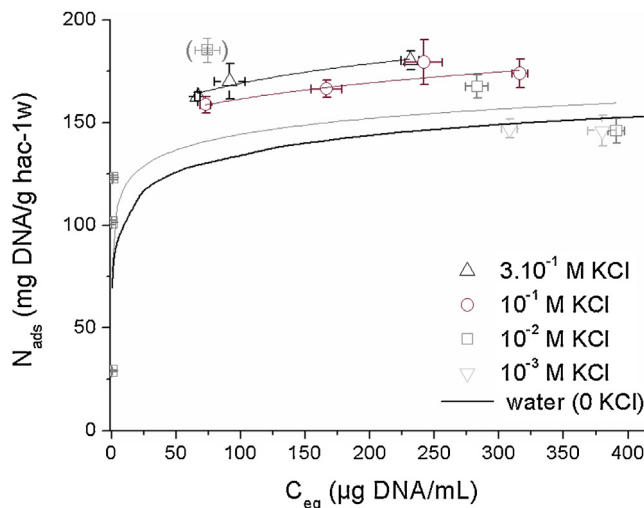


**Fig. 7.** Effect of ionic strength on DNA adsorption with increasing amount of KCl (0–300 mM) in standard conditions.

In the diagenetic context, our observations of the role of pH on the adsorbed DNA amounts on biomimetic apatite may incite one to hastily conclude on a “positive” effect of acidic environments on DNA preservation; however it should be kept in mind that apatitic substrates are bound to degrade faster in such conditions, thus not favoring long-term DNA preservation [17,50].

### 3.3.4. Role of ionic strength

The influence of the overall salinity of the solution (varied here by incorporation of various amounts of KCl in the adsorption medium, with  $[KCl] = 1\text{--}300\text{ mM}$ ) was also checked at 22 °C. Indeed, ionic strength is another parameter likely to influence adsorption processes [51], as well as DNA decay [52]. The obtained data (see main trends on Fig. 7) indicate a clear tendency toward increasing DNA adsorbed amounts when increasing the ionic strength of the medium.

These findings could be linked to a decrease in inter-molecular interaction, thus facilitating the adsorption process onto apatite crystals surfaces. Again, a variation in DNA conformation may play a role in these observations. The impact of the concentration in DNA of a given solution on its conformation and on molecular inter-penetration was addressed in past studies [53,54]. In the present case – as well as in usual diagenetic processes – the density of DNA molecules is however expected to be rather limited, thus corresponding to “dilute” systems rather than highly concentrated ones: in these conditions, each molecule may thus have a tendency to act as a separate entity, as suggested by Tomic et al. [54]. It should also be added that the “critical role of counter-ion valence in modulating inter-polyion forces” has been recently underlined, especially in the case of DNA macromolecules [54–56]. This may thus complicate further the understanding and modeling of DNA molecular dynamics under modified salinity conditions; and additional data are probably needed on this field prior to draw mechanistic conclusions on the effect of ionic strength on DNA conformation and consequently on adsorption. Nevertheless, our experimental data, obtained in the presence of KCl, point out a measurable impact on adsorption capabilities of DNA on biomimetic apatite, thus suggesting that salinity should be considered as a non-negligible influential parameter in such adsorption processes.

### 3.3.5. Role of temperature

The effect of temperature on DNA adsorption on the hac-1w sample was then examined. In view of shedding some light on

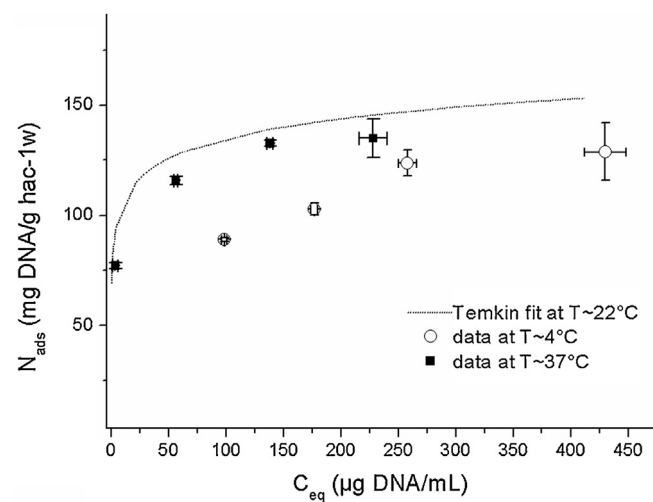


**Fig. 8.** Effect of temperature on DNA equilibrium adsorption of at 4 °C (5 d incubation) and at 37 °C (3 d incubation). For comparison, the Temkin fit at room temperature is also shown

the effect of temperature on DNA adsorption on apatite, datapoints were obtained at three temperatures covering a wide range between body temperature and near-permafrost temperature, namely 37, 22 and 4 °C and the results are reported in Fig. 8. As may be noticed, the values of  $N_{ads}$  obtained at 22 or 37 °C do not differ drastically, in contrast to data corresponding to 4 °C. Such “cold” conditions (during the adsorption process) indeed lead to noticeably lower amounts of adsorbed DNA, for a given DNA concentration at equilibrium. The isotherm obtained at 4 °C also appears to display a different profile compared to “warmer” conditions, and linearization tests corresponding to the Temkin, Freundlich or Langmuir models indicated in this case a better correlation with the latter model (correlation coefficient  $R^2 = 0.8515$  for Langmuir as opposed to 0.7832 and 0.7583 respectively for Freundlich and Temkin). This observation then points out some modifications in the type of molecule/molecule and/or of molecule/substrate interactions in such a colder situation. It is however difficult, at this stage, to propose a more advanced modeling for this phenomenon as additional information would be needed for instance on the evolution of the surface reactivity (e.g. exchangeability of  $HPO_4^{2-}$  surface ions) of apatitic substrates versus temperature.

## 4. Concluding remarks

The present contribution aimed at shedding some light, for the first time on a physico-chemical point of view, on the type of interaction existing between biomimetic apatites and DNA macromolecules, or relevance both in forensic and anthropologic contexts.

Our experimental findings strongly support the general empirical hypothesis, often emitted in the ancient DNA community, after which DNA strands could interact with apatite found in hard tissues thus considerably limiting its degradation with time. The study of the kinetics of DNA adsorption on a synthetic biomimetic apatite sample showed that the data could be adequately fitted to an Elovichian equation, often found for rather slow adsorption processes. The shape of the adsorption isotherms obtained in various conditions was found to be satisfactorily described by the Temkin model (except at low temperature). The effect of pH, ionic strength and temperature on the adsorbed amounts has been explored, suggesting the non-negligible role of environmental parameters

(at least during the adsorption stage). Although a “simple” dilution of the medium did not provoke the desorption of DNA, thus suggesting a strong binding affinity of DNA for apatitic surfaces, the addition of phosphate ions was found to promote the release of the macromolecules (pointing out a competition for surface sites between DNA phosphate groups and inorganic phosphate ions).

This study is intended to help understanding diagenetic processes undergone by DNA in skeletal remains, and also to better apprehend the interactions that DNA may undertake with apatitic substrates from which it is retrieved. More advanced knowledge on such interactions may also allow one to optimize, in turn, DNA extraction procedures.

The dedicated analysis of the solids after DNA adsorption and the exploration of the interaction of shorter DNA fragments with apatitic substrates represent upcoming perspectives for this work, and will be the object of future complementary studies.

## Acknowledgements

This research was supported by the Institute of Ecology and Environment (INEE) and the Institute of Chemistry (INC) of the French National Centre for Scientific Research (CNRS).

## References

- [1] T. Delabarde, C. Keyser, A. Tracqui, D. Charabidze, B. Ludes, The potential of forensic analysis on human bones found in riverine environment, *Forensic Sci. Int.* 228 (2013) e1–e5.
- [2] C. Keyser, C. Bouakaze, E. Crubézy, V.G. Nikolaev, D. Montagnon, T. Reis, et al., Ancient DNA provides new insights into the history of south Siberian Kurgan people, *Hum. Genet.* 126 (2009) 395–410.
- [3] C. Keyser-Tracqui, B. Ludes, Methods for the study of ancient DNA, *Methods Mol. Biol.* 297 (2005) 253–264.
- [4] N. Nassif, F. Martineau, O. Syzgantseva, F. Gobeaux, M. Willinger, T. Coradin, et al., In vivo inspired conditions to synthesize biomimetic hydroxyapatite, *Chem. Mater.* 22 (2010) 3653–3663.
- [5] A.S. Posner, F. Betts, Synthetic amorphous calcium phosphate and its relation to bone mineral structure, *Acc. Chem. Res.* 8 (1975) 273–281.
- [6] C. Rey, Calcium phosphate biomaterials and bone mineral. Differences in composition, structures and properties, *Biomaterials* 11 (1990) 13–15.
- [7] E.D. Eanes, J.L. Meyer, The maturation of crystalline calcium phosphates in aqueous suspensions at physiologic pH, *Calcif. Tissue Res.* 23 (1977) 259–269.
- [8] C. Rey, A. Hina, A. Tofighi, M.J. Glimcher, Maturation of poorly crystalline apatites: chemical and structural aspects in vivo and in vitro, *Cells Mater.* 5 (1995) 345–356.
- [9] C. Rey, J. Lian, M. Grynpas, F. Shapiro, L. Zylberberg, M.J. Glimcher, Non-apatitic environments in bone mineral: FT-IR detection, biological properties and changes in several disease states, *Connect. Tissue Res.* 21 (1989) 267–273.
- [10] S. Cazalbou, D. Eichert, X. Ranz, C. Drouet, C. Combes, M.F. Harmand, et al., Ion exchanges in apatites for biomedical application, *J. Mater. Sci. Mater. Med.* 16 (2005) 405–409.
- [11] F. Errassifi, A. Menbaoui, H. Autefage, L. Benaziz, S. Ouizat, V. Santran, et al., Adsorption on apatitic calcium phosphates: applications to drug delivery, in: R. Narayan, J. McKittrick (Eds.), *Advances in Bioceramics and Biotechnologies*, American Ceramic Society, Westerville, 2010, pp. 159–174.
- [12] S. Ouizat, A. Barroug, A. Legrouri, C. Rey, Adsorption of bovine serum albumin on poorly crystalline apatite: influence of maturation, *Mater. Res. Bull.* 34 (1999) 2279–2289.
- [13] A.S. Posner, The structure of bone apatite surfaces, *J. Biomed. Mater. Res.* 19 (1985) 241–250.
- [14] S. Cazalbou, C. Combes, D. Eichert, C. Rey, M.J. Glimcher, Poorly crystalline apatites: evolution and maturation in vitro and in vivo, *J. Bone Miner. Metab.* 22 (2004) 310–317.
- [15] N. Vandecandelaere, C. Rey, C. Drouet, Biomimetic apatite-based biomaterials: on the critical impact of synthesis and post-synthesis parameters, *J. Mater. Sci. Mater. Med.* 23 (2012) 2593–2606.
- [16] M.J. Collins, C.M. Nielsen-Marsh, J. Hiller, C.I. Smith, J.P. Roberts, R.V. Prigodich, et al., The survival of organic matter in bone: a review, *Archaeometry* 44 (2002) 383–394.
- [17] T. Lindahl, Instability and decay of the primary structure of DNA, *Nature* 362 (1993) 709–715.
- [18] N. Tuross, The biochemistry of ancient DNA in bone, *Experientia* 50 (1994) 530–535.
- [19] L. Orlando, A. Ginolhac, G. Zhang, D. Froese, A. Albrechtsen, M. Stiller, et al., Recalibrating Equus evolution using the genome sequence of an early Middle Pleistocene horse, *Nature* 499 (2013) 74–78.
- [20] G. Bernardi, Chromatography of nucleic acids on hydroxyapatite, *Nature* 206 (1965) 779–783.
- [21] R.K. Main, M.J. Wilkins, L.J. Cole, Partial chromatographic separation of pentose- and deoxypentose nucleic acids, *Science* 129 (1959) 331–332.
- [22] T. Watanabe, K. Makitsuru, H. Nakazawa, S. Hara, T. Suehiro, A. Yamamoto, et al., Separation of double-strand DNA fragments by high-performance liquid chromatography using a ceramic hydroxyapatite column, *Anal. Chim. Acta* 386 (1999) 69–75.
- [23] F.L. Graham, A.J. van der Eb, A new technique for the assay of infectivity of human adenovirus 5 DNA, *Virology* 52 (1973) 456–467.
- [24] M. Jordan, A. Schallhorn, F.M. Wurm, Transfecting mammalian cells: optimization of critical parameters affecting calcium-phosphate precipitate formation, *Nucleic Acids Res.* 24 (1996) 596–601.
- [25] M. Okazaki, Y. Yoshida, S. Yamaguchi, M. Kaneno, J.C. Elliott, Affinity binding phenomena of DNA onto apatite crystals, *Biomaterials* 22 (2001) 2459–2464.
- [26] H. Autefage, F. Briand-Mésange, S. Cazalbou, C. Drouet, D. Fourmy, S. Gonçalvès, et al., Adsorption and release of BMP-2 on nanocrystalline apatite-coated and uncoated hydroxyapatite/β-tricalcium phosphate porous ceramics, *J. Biomed. Mater. Res. B: Appl. Biomater.* 91B (2009) 706–715.
- [27] L. Benaziz, A. Barroug, A. Legrouri, C. Rey, A. Lebugle, Adsorption of O-phospho-L-serine and L-serine onto poorly crystalline apatite, *J. Colloid Interface Sci.* 238 (2001) 48–53.
- [28] D.N. Misra, Adsorption and orientation of tetracycline on hydroxyapatite, *Calcif. Tissue Int.* 48 (1991) 362–367.
- [29] P. Pascaud, P. Gras, Y. Coppel, C. Rey, S. Sarda, Interaction between a bisphosphonate, tiludronate, and biomimetic nanocrystalline apatites, *Langmuir* 29 (2013) 2224–2232.
- [30] H. Tanaka, K. Miyajima, M. Nakagaki, S. Shimabayashi, Incongruent dissolution of hydroxyapatite in the presence of phosphoserine, *Colloid Polym. Sci.* 269 (1991) 161–165.
- [31] A. Gee, V.R. Deitz, Determination of phosphate by differential spectrophotometry, *Anal. Chem.* 25 (1953) 1320–1324.
- [32] R. Legros, *Apport de la physico-chimie à l'étude de la phase minérale des tissus calcifiés* (Thèse d'Etat), Institut national polytechnique, 1984.
- [33] M.J.D. Low, Kinetics of chemisorption of gases on solids, *Chem. Rev.* 60 (1960) 267–312.
- [34] C. Aharoni, F.C. Tompkins, Kinetics of adsorption and desorption and the Elovich equation, in: H. Pines, P.B. Weisz, D.D. Eley (Eds.), *Advances in Catalysis*, Academic Press, 1970, pp. 1–49.
- [35] F.-C. Wu, R.-L. Tseng, R.-S. Juang, Characteristics of Elovich equation used for the analysis of adsorption kinetics in dye–chitosan systems, *Chem. Eng. J.* 150 (2009) 366–373.
- [36] J.M. Thomas, W.J. Thomas, *Principles and Practice of Heterogeneous Catalysis*, VCH, New York, USA, 1996.
- [37] C. Cheung, J. Porter, G. McKay, Sorption kinetic analysis for the removal of cadmium ions from effluents using bone char, *Water Res.* 35 (2001) 605–612.
- [38] A.G. Ritchie, Alternative to the Elovich equation for kinetics of adsorption of gases on solids, *J. Chem. Soc. Faraday Trans.* 73 (1997) 1650–1653.
- [39] L. Sciascia, M.L. Turco Liveri, M. Merli, Kinetic and equilibrium studies for the adsorption of acid nucleic bases onto K10 montmorillonite, *Appl. Clay Sci.* 53 (2011) 657–668.
- [40] J.O. Bockris, K.T. Jeng, In-situ studies of adsorption of organic compounds on platinum electrodes, *J. Electroanal. Chem.* 330 (1992) 541–581.
- [41] G. Skodras, I. Diamantopoulou, G. Pantoleontos, G.P. Sakellaropoulos, Kinetic studies of elemental mercury adsorption in activated carbon fixed bed reactor, *J. Hazard. Mater.* 158 (2008) 1–13.
- [42] S. Trasatti, L. Formaro, Kinetics and mechanism of the adsorption of glycolaldehyde on a smooth platinum electrode, *J. Electroanal. Chem. Interfacial Electrochem.* 17 (1968) 343–364.
- [43] M.A. Vannice, *Kinetics of Catalytic Reactions*, Springer, New York, 2005.
- [44] F. Errassifi, Mécanismes d'adsorption du risédronate par des phosphates de calcium biologiques: applications aux biomatériaux, Faculté des Sciences Semlalia-Marrakech, 2011.
- [45] J.C. Elliott, *Structure and Chemistry of the Apatites and Other Calcium Orthophosphates*, Elsevier Science & Technology, Amsterdam, 1994.
- [46] C. Rey, M. Shimizu, B. Collins, M.J. Glimcher, Resolution-enhanced Fourier transform infrared spectroscopy study of the environment of phosphate ion in the early deposits of a solid phase of calcium phosphate in bone and enamel and their evolution with age: 2. Investigations in the  $\nu_3 \text{PO}_4$  domain, *Calcif. Tissue Int.* 49 (1991) 383–388.
- [47] C. Rey, M. Shimizu, B. Collins, M.J. Glimcher, Resolution-enhanced Fourier transform infrared spectroscopy study of the environment of phosphate ions in the early deposits of a solid phase of calcium-phosphate in bone and enamel, and their evolution with age. I. Investigations in the  $\nu_4 \text{PO}_4$  domain, *Calcif. Tissue Int.* 46 (1990) 384–394.
- [48] J.A.V. Butler, *Progress in Biophysics and Biophysical Chemistry*, Pergamon Press, London, 1951.
- [49] G. Charlot, *L'analyse qualitative et les réactions en solution*, Masson, Paris, France, 1963.
- [50] R. Bollongino, A. Tresset, J.-D. Vigne, Environment and excavation. Pre-lab impacts on ancient DNA analyses, *C. R. Palevol.* 7 (2008) 91–98.
- [51] D.N. Misra, *Adsorption on and Surface Chemistry of Hydroxyapatite*, Springer, New York, 1984.
- [52] T. Lindahl, B. Nyberg, Rate of depurination of native deoxyribonucleic acid, *Biochemistry (Mosc.)* 11 (1972) 3610–3618.

- [53] A.V. Dobrynin, M. Rubinstein, Theory of polyelectrolytes in solutions and at surfaces, *Prog. Polym. Sci.* 30 (2005) 1049–1118.
- [54] S. Tomić, D. Grgićin, T. Ivec, T. Vuletić, S. Dolanski Babić, R. Podgornik, Dynamics and structure of biopolyelectrolytes in repulsion regime characterized by dielectric spectroscopy, *Phys. B: Condens. Matter* 407 (2012) 1958–1963.
- [55] A. Naji, M. Kanduc, R.R. Netz, R. Podgornik, Exotic electrostatics: unusual features of electrostatic interactions between macroions, ArXiv Prepr, 2010 arXiv:1008.0357.
- [56] R.W. Wilson, V.A. Bloomfield, Counterion-induced condensation of deoxyribonucleic acid. A light-scattering study, *Biochemistry (Mosc.)* 18 (1979) 2192–2196.